LHC Project Note 364

2005-01-26

Andrew.Presland@cern.ch

Thijs.Wijnands@cern.ch

Radiation levels in UJ32 during nominal LHC operation.

Andrew Presland AB/ATB/EET, Thijs Wijnands TS/LEA

Keywords: radiation, dose, shielding, UJ32, beam-gas

Summary

This report presents estimated radiation levels inside the UJ32 under nominal LHC running conditions. The radiation levels are expressed in terms of total dose [Gy], 1MeV neutrons equivalent fluence and the fluence of hadrons having energy in excess of 20 MeV. When the average loss rate around the ring is $1.65\times10^{11}m^{-1}y^{-1}$ the annual dose inside an electronics rack in UJ32 is 1×10^{-2} Gy [Si], the annual 1 MeV eq. Neutron fluence is 5×10^{8} per cm^2 and the annual high energetic hadron fluence is 5×10^{7} per cm^2.

1. Introduction

The aim of this study is to provide estimations of the radiation levels seen by electronics situated within UJ32 (Figure 1) situated within Arc23 opposite half-cell 18L3. Radiation in this area is mainly caused by inelastic interactions of the circulating proton beams with the residual gas in the vacuum chamber of the LHC. The cascades originate from two main sources: point losses downstream of the high luminosity interaction points and insertion regions and from beam-gas interactions. Point losses occur when off-momentum protons that have left the stable phase-space interact with nuclei of any material surrounding the beams such as the beam-screen, collimators, magnets or cables. Radiation from beam-gas interactions occurs when secondary particles, emitted by a nuclear inelastic interaction with a nucleus of the residual gas in the vacuum chamber, are swept out of the beam axis by the magnetic field of the bending magnets (charged particles) or go straight (neutral particles) and touch the vacuum chamber downstream of the primary interaction (up to approximately 15m). Hadronic cascades may produce secondary particles with sufficient momentum to reach electronic equipment within UJ32.

The hadronic cascade simulations were performed using the Monte-Carlo particle shower code FLUKA [Fas93], [Fas94], [Fas97a], [Fas97b], [Fer96]. The UJ32 geometry description includes the entrance chicane and the area with electronics racks behind. It will be shown in the next sections that the dose rate at the UJ32 entrance (tunnel side) is a typically a few Gy per year and similar to that in the Arc extending to the tunnel wall [Pot95b],[Huh96]&[Fyn00].

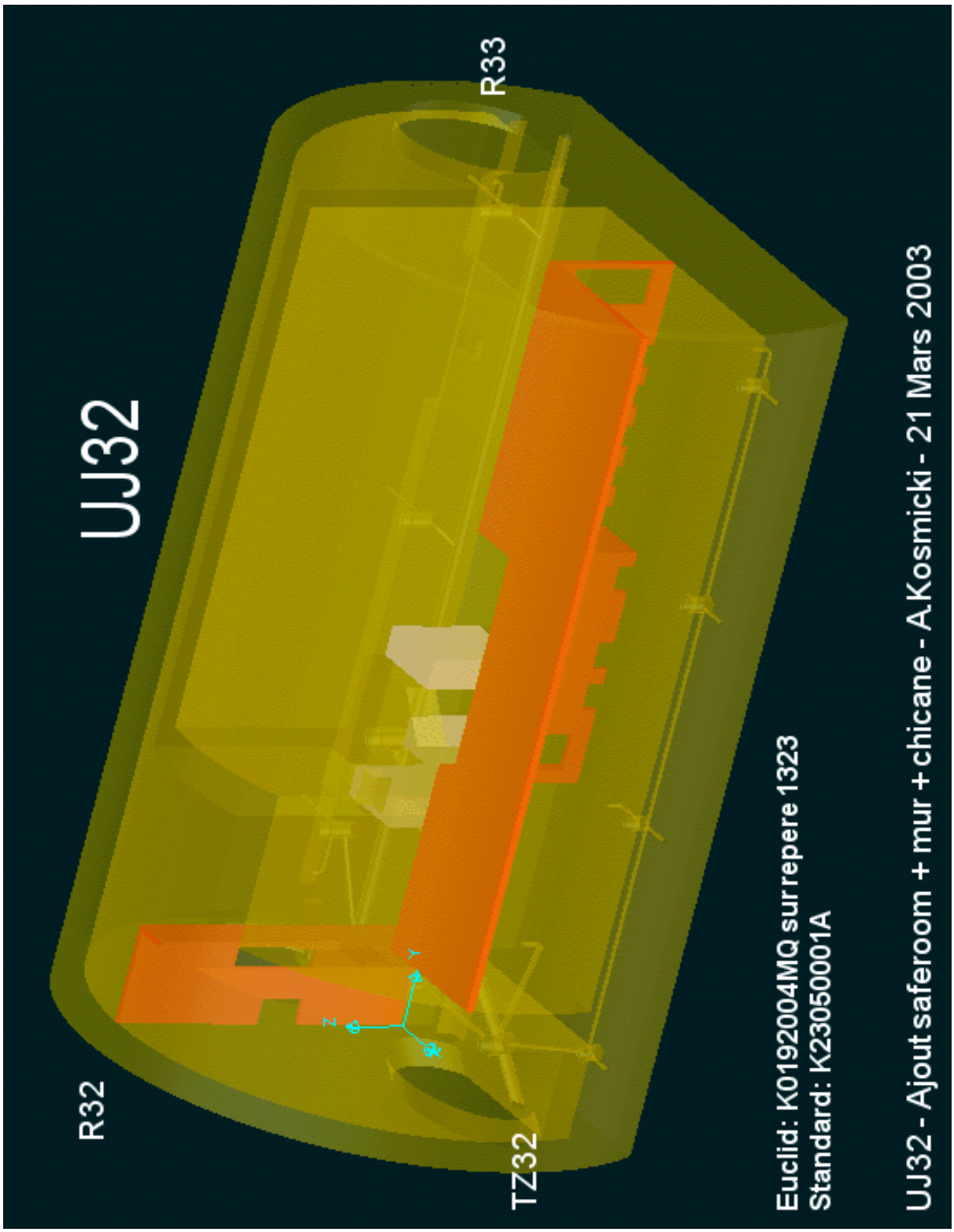

Figure 1. 3D view of UJ32 showing original concrete structure (green), additional walls (orange) and shielding stacks (grey).

2. Radiation sources.

2.1 Beam Gas interactions

The number of beam-gas interactions depends on the molecular composition of the gas estimates of these values have become more precise during the last few years. The limiting value of beam-gas interaction rate can be deduced from the maximum heat load in the main cryo magnets in the rings. Alternatively, the interaction rate can be estimated from physics operations and the envisaged operational scenarios.

The results presented here assume a value of beam-gas interaction rates of 1.65×10^{11} $m^{-1}y^{-1}$ ($1.05\times10^{4}m^{-1}s^{-1}$) [Pot95a] Pot95b]. This value was used in the past by Stevenson and Fynbo to compute the radiation levels in the regular ARCs and is derived from the limiting value of cryogenic load coming from heating by hadronic showers assuming a 250 hour beam-gas lifetime limit. The H_2 equivalent gas density for a 250 hours beam-gas lifetime is 2.5×10^{15} molecules/m^3.

2.2 Point Losses

The point loss distribution around the ring has local maxima at the high luminosity interaction points IP1 and IP5 and in the collimation insertion regions IR3 and IR7.

In the Arc23, contributions to annual radiation levels could arise from off-momentum protons created in the high luminosity interaction point IP1. However, detailed calculations [Fyn01] have shown a negligible contribution to the dose rates beyond quadrupole QF19 in the adjacent arcs (Arc12, Arc81).

Another contribution could arise from off-momentum protons created in the momentum cleaning insertion IR3 leading to down stream point losses. Estimates made by [Bai] show however, that the downstream proton losses are concentrated in the chain of Dispersion Suppressor (DS) magnets B8B-Q8-B9A.

In very good approximation we can therefore neglect all contributions to the radiation levels in UJ32 from point losses.

3. Existing Shielding

All equipment in UJ32 is shielded by a minimum of 100 cm of concrete provided by the main internal wall. The wall is punctured by a chicane providing access whilst ensuring all straight line paths offer full shield coverage. This configuration will significantly reduce the dose from electromagnetic showers (including pi0) and diminish charged hadron fluence. The neutron multiplicity will be increased as charged hadrons induce spallation and nuclear evaporation but the energy of these and primary neutrons will be moderated by elastic scattering inside the concrete. Concrete will therefore reduce the neutron damage.

A chicane is required because low energy neutrons in air channels (such as the entrance passage) are particularly troublesome. They readily scatter from the wall and can propagate down the passage in a series of ‘reflections’ even if the channel is not in the original direction of the neutron. Fortunately the scattering of neutrons implies that neutron flow does not readily turn corners and the chicane acts therefore as a neutron trap. The shielding chicane still allows access for services and/or personnel to the alcove whilst containing the neutron fluence.

4. FLUKA Monte Carlo Simulation

4.1 Geometry

Since UJ32 is positioned alongside standard Arc23 the methodology of previous studies can be used to obtain dose estimates in the arc sections and the geometry enlarged to include the civil engineering of UJ32. The full FLUKA geometry for the LHC ARC section consists of six main bending dipole magnets (MBA/MBB), the quadrupole (MQ) and their correcting magnets. The geometry is setup according to LHC design optics 6.2 which is the same geometry as used in the earlier studies of dose in the arc sections [Fyn01]. More recent version (V6.5) of the LHC optics do not lead to significantly different results as the ARC section 2-3 in these versions is identical to version V6.2.

The extension of this geometry to include the UJ32 civil works is shown in figures 3-5.

For location of scoring bins please refer to section 5.

4.2 Monte Carlo methodology

The following methodology was used for performing the Monte Carlo simulation:

- First 7 TeV protons were forced to interact with an isotropic distribution along the beam line. In total 20.000 interactions were simulated. Interactions are forced with carbon nuclei since these dominate the cross-section for beam-gas interactions. The effect of including the true gas composition on results is small but greatly complicates the simulation.

- The dose (hadron fluence, 1 MeV Equiv) in a scoring bin is then given by the sum of all contributions scored in that bin arising from each of the interactions. This data is then normalised to give the dose (hadron fluence, 1 MeV Equiv) per interacting proton in the beam line.

- Final results are obtained by weighting the data per interacting by the appropriate proton loss rate due to beam-gas interactions.

The total energy deposition (GeV) is converted to dose (1 Gy = 1 J/Kg) and normalised to the given proton loss per year – giving annual dose per year in each scoring bin. The total fluence is converted to a 1MeV neutron equivalent fluence on a particle-by-particle basis by interpolating between the values of NIEL curve data. The 20MeV hadron fluence is obtained by applying a threshold to the hadron fluence.

4.3 Monte Carlo error sources

Many sources contribute to the overall uncertainties in the simulated levels [Huh00]. Amongst these are the inelastic *pp* cross section at 7 TeV, the uncertainty in the event structure, energy flow and multiplicity as a function of rapidity. The influence of these effects on the results has been studied by comparing event generators and a variation of a factor 1.3 was observed [Huh95]. Furthermore a factor 2 caused by the geometry description and material composition is customary. It remains an open question how accurately the FLUKA code can predict the radiation environment. A study presented in [Huh00] has approached this problem by comparing the results of FLUKA and MARS codes in a simple, well defined geometry. This test will not be affected by experimental errors and since the two codes are independent they should not contain the same errors. This yielded almost perfect agreement for energy-integrated

neutron fluxes and for energy deposition and good agreement in the charged hadron spectra and this error can be neglected.

It is a paradox that if a shielding design is effective it will limit the statistical accuracy in that region in which we have most concern. Fortunately we can use statistical biasing in order to reduce the impact of this paradox on results. In this study the multiplicity of secondary particles has been biased using importance sampling. Vertical biasing planes parallel to the beam line define biasing regions in areas of strong attenuation (mainly concrete). Particle splitting is performed at each boundary crossing and the particle weight adjusted. The amount of splitting depends on the ratio of bias weights on either side of the plane. The final result is that the particle fluence is enhanced in shielded areas with an associated improvement in scoring statistics.

To good approximation we can therefore ignore the statistical error contribution and the results presented here have a factor 2 cumulated error.

5. Simulation Results

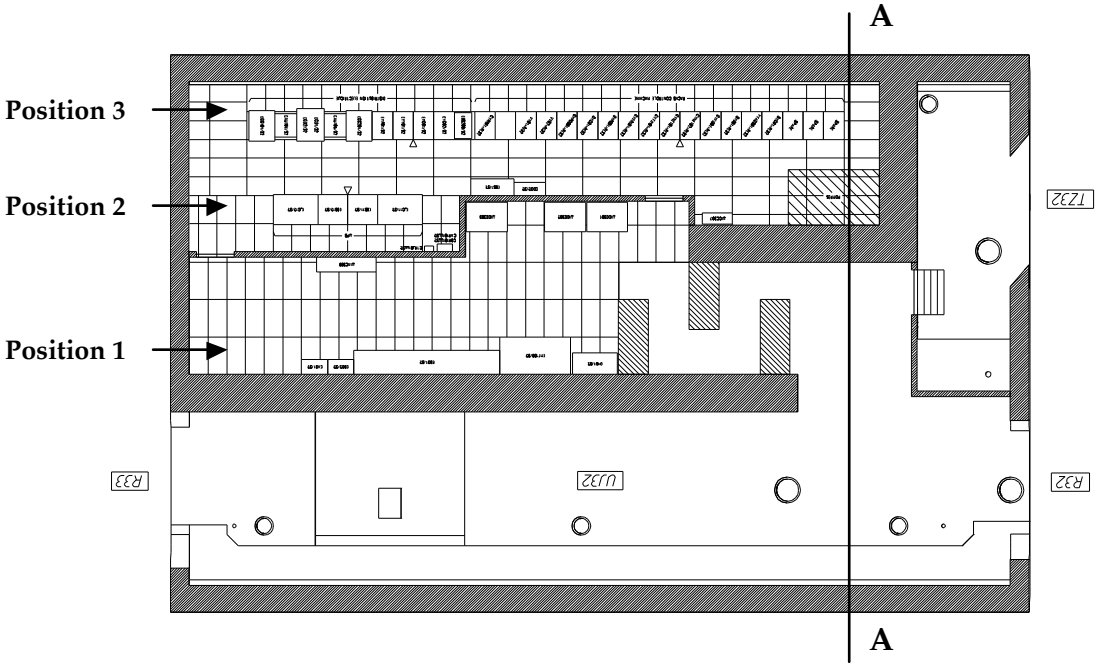

Figure 2. UJ32 floor-plan showing the proposed positions of electronics racks and sectional cut A-A used in scoring of radiation levels.

Results were scored in meshes of 20×20×50 cm^3 bin size inside UJ32: a horizontal mesh at the level of the beam pipe inside UJ32, a horizontal mesh at 95 cm above the upper floor level of UJ32, and a vertical mesh forming a transverse a scoring at the position indicated in figure 2 by section A-A.

The total energy deposition (GeV) is converted to dose (1 Gy = 1 J/Kg) and normalised to the given proton loss per year – giving annual dose per year in each scoring bin. The total fluence is converted to a 1MeV neutron equivalent fluence on a particle-by-particle basis by interpolating between the values of NIEL curve data. The 20MeV hadron fluence is obtained by applying a simple threshold to the hadron fluence.

5.1 Total Ionising Dose

The expected annual dose inside UJ32 is shown in Figure 3. With reference to Figure 2 it can be seen that annual doses below or in the order of $1x10^{-2}$ Gy per year are to be anticipated at all positions where electronics crates have to be positioned. This dose rate presents no reason for concern for electronics damage.

5.2 Highly Energetic Hadron Fluence

The expected annual fluence of hadrons with energy in excess of 20 MeV inside UJ32 is shown in Figure 4. With reference to Figure 2 it can be seen that annual fluences tabulated below have to be anticipated at the electronics racks positions.

Table 1. 20 MeV hadron fluence in hadrons $cm^{-2}y^{-1}$ due to beam-gas interactions.

	Position 1	**Position 2**	**Position 3**
20 MeV hadron fluence	$1x10^{8}$	$5x10^{7}$	$1x10^{7}$

A high energy hadron flux of 1x108 cm-2y-1 may be of concern for electronics that is using biased memory or power electronics.

5.3 Estimates of 1 MeV Neutrons Equivalent Fluence

The expected annual 1 MeV neutrons equivalent fluence expected inside UJ32 is shown in Figure(5. With reference to Figure 2 it can be seen that annual 1 MeV neutrons equivalent fluences tabulated below can be anticipated at the electronics racks positions.

Table 2. 1 MeV equivalent neutron fluence in neutrons $cm^{-2}y^{-1}$ due to beam-gas interactions.

	Position 1	**Position 2**	**Position 3**
1 MeV Equiv. Fluence	$1x10^{9}$	$5x10^{8}$	$1x10^{8}$

As most electronics components can withstand such a fluence this is only of minor concern.

6. Summary

Review of previous studies has shown that proton losses inside Arc23 are dominated by beam-gas interactions and the contributions from point losses can be neglected. The radiation levels inside UJ32 have been simulated with FLUKA using both the interaction rate compatible with that derived from the expected H2 equivalent gas density limit (1×10^{15} molecules/m3).

For the UJ32 geometry considered main shielding wall provides a reduction of the hadron and 1 MeV neutron equivalent fluence of a factor 10. A reduction approaching a factor 100 is obtained for total ionizing dose. The entrance chicane is seen to effectively trap neutrons that would otherwise propagate into the equipment area.

In general, the radiation levels in each quantity of interest in all areas on the non-beam side of the main shielding wall are distributed within an order of magnitude. The annual dose will be

below 0.01 Gy/y. The annual fluence of hadrons with energy in excess of 20 MeV is expected to range from 10^8 hadrons $cm^{-1}y^{-1}$ for positions closest to the beam to 10^7 hadrons $cm^{-1}y^{-1}$ for positions furthest from the beam and the 1 MeV neutrons equivalent fluence is expected to range from 10^9 neutrons $cm^{-2}y^{-1}$ to 10^8 neutrons $cm^{-2}y^{-1}$ for positions furthest from the beam.

At this level dose is not an issue and electronics in all equipment areas are expected to operate within specification during nominal operation. High energetic neutrons may be a problem for the power distribution racks close to the beam. The neutron flux monitoring equipment that will be installed at the chicane entry, will help to make this issue more precise.

References

[Fas93] A. Fasso, A.Ferrari, J. Ranft and P.R. Sala, *FLUKA: present status and future developments,* Proc IV Int. Conf. On Calorimetry in High Energy Physics, La Biodola (Isola d'Elba), Sept. 20-25 1993. Ed. A. Mezione and A. Scribano, World Scientific, p 493 (1993).

[Fas94] A. Fasso, A.Ferrari, J. Ranft and P.R. Sala, *FLUKA: Performances and Applications in the Intermediate Energy Range*, Specialists' Meeting on Shielding Aspects of Accelerators, Targets and Irradiation Facilities. Arlington, Texas, April 28-29 1994, NEA/OECD (Paris) p. 287.

[Fas97a] A. Fass` o, A. Ferrari, J. Ranft and P. R. Sala, *An update about FLUKA*, Proc. 2nd Workshop on Simulating Accelerator Radiation Environments, CERN, Geneva, Switzerland 9-11 Oct. 1995, Ed. G.R. Stevenson, CERN Report TIS-RP/97-05, p.158-170.

[Fas97b] A. Fass` o, A. Ferrari, J. Ranft and P. R. Sala, *New developments in FLUKA modelling hadronic and EM interactions*, Proc. 3rd Workshop on Simulating Accelerator Radiation Environments, KEK, Tsukuba, Japan 7-9 May 1997, Ed. H. Hirayama, KEK Proceedings 97-5, p.32-43.

[Fer96] A. Ferrari and P. R. Sala, *The Physics of High Energy Reactions*, in Proceedings of the Workshop on Nuclear Reaction Data and Nuclear Reactors Physics, Design and Safety, International Centre for Theoretical Physics, Miramare-Trieste, Italy, 15 April - 17 May 1996, Ed. A. Gandini and G. Reffo, World Scientific, p.424 (1998).

[Fyn00] C. A. Fynbo and G. R. Stevenson, *The ratio of doses to neutron and hadron fluences for components exposed to LHC beam-gas interactions*, EST Technical Note EST-LEA/2000-001.

[Huh96] M. Huhtinen and G. R. Stevenson, *Doses around the LHC beam-pipe due to beam-gas interactions in a long straight section*, CERN-LHC Project Note 39 (1996).

[Pot95a] K. Potter and G. R. Stevenson, *Source intensities for use in the radiological assessment of the effect of proton losses at the scrapers and around the main ring of the LHC*, CERN Internal Report TIS–RP/IR/95–16 (1995), CERN AC/95–04(DI), LHC Note 322.

[Pot95b] K. Potter, H. Sch¨onbacher and G. R. Stevenson, *Estimates of dose to components in the arcs of the LHC due to beam-loss and beam-gas interactions*, CERN-LHC Project Note 18 (1995).

[Ste00] G. R. Stevenson and C. A. Fynbo, *The LHC-machine radiation environment*, Presented at the CERN TECHNICAL TRAINING meeting on Radiation Effects on Electronic Components and Systems for LHC, held 10-12 April 2000. Can be obtained under 'CERN Courses on Radiations' under the Radiation Working Group (RADWG) web page.

[Huh00] M. Huhtinen and N. V. Mokhov, *A Cross-comparison of MARS amd FLUKA Simulation Codes*, FERMILAB-FN-697.

[Huh95] M. Huhtinen and C. Seez, CERN CMS TN95-133(1995).

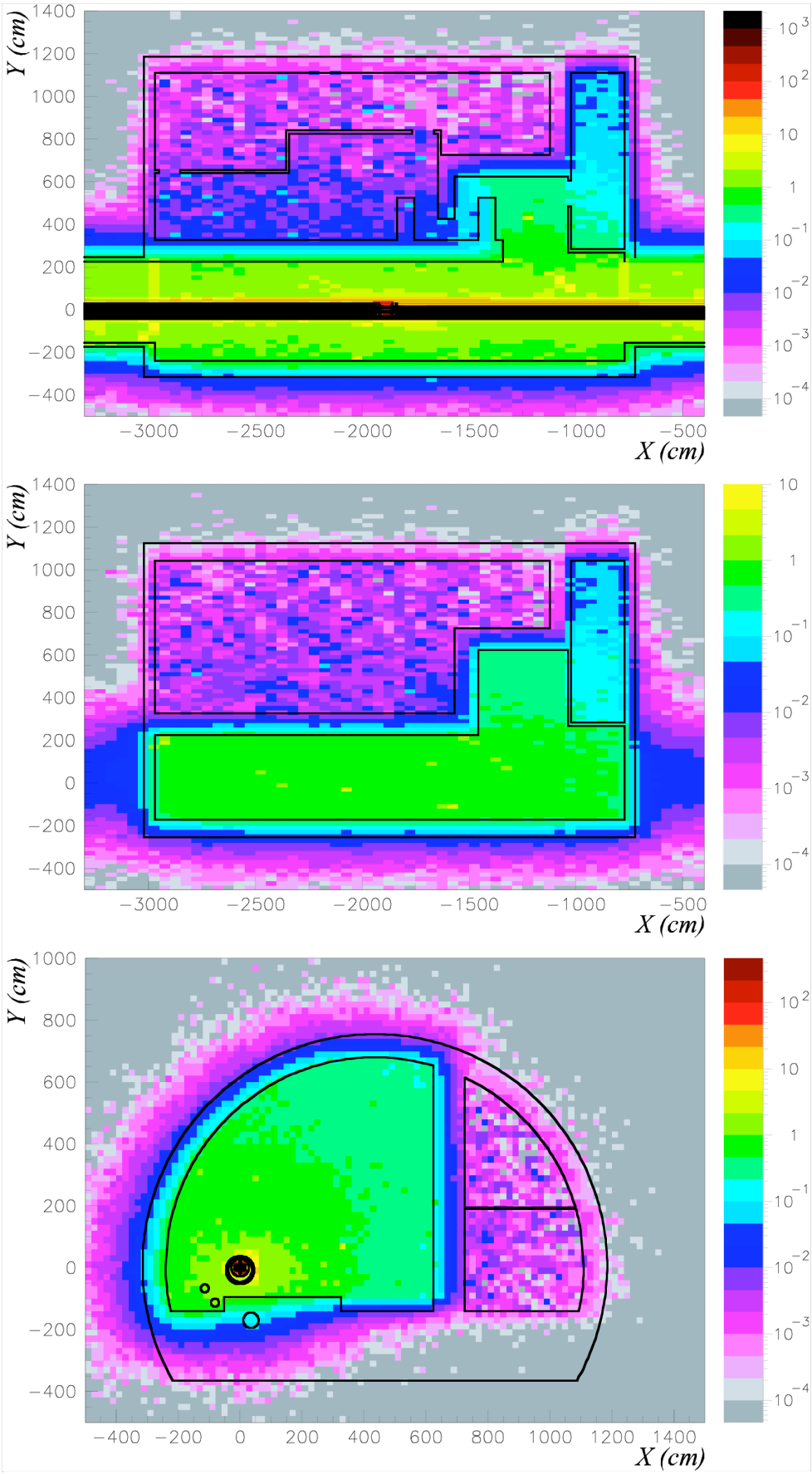

Figure 3. Annual dose in UJ32. Horizontal cuts averaged over 20 cm about a plane 95 cm above floor levels and vertical cut averaged over 20 cm about section indicated in figure 2.

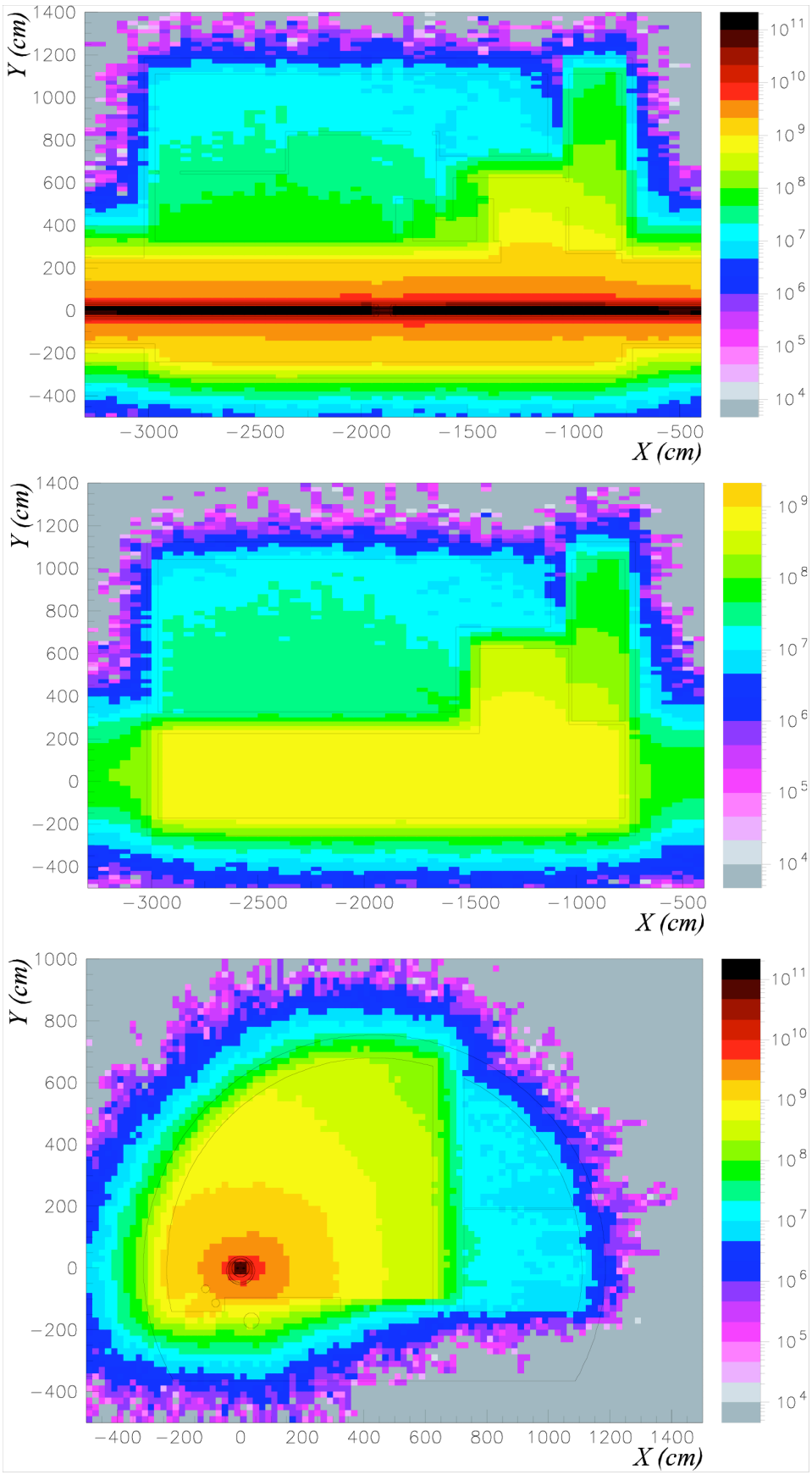

Figure 4 Annual fluence of hadrons with energy in excess of 20 MeV. Horizontal cuts averaged over 20 cm about a plane 95 cm above floor levels and vertical cut averaged over 20 cm about section indicated in figure 2.

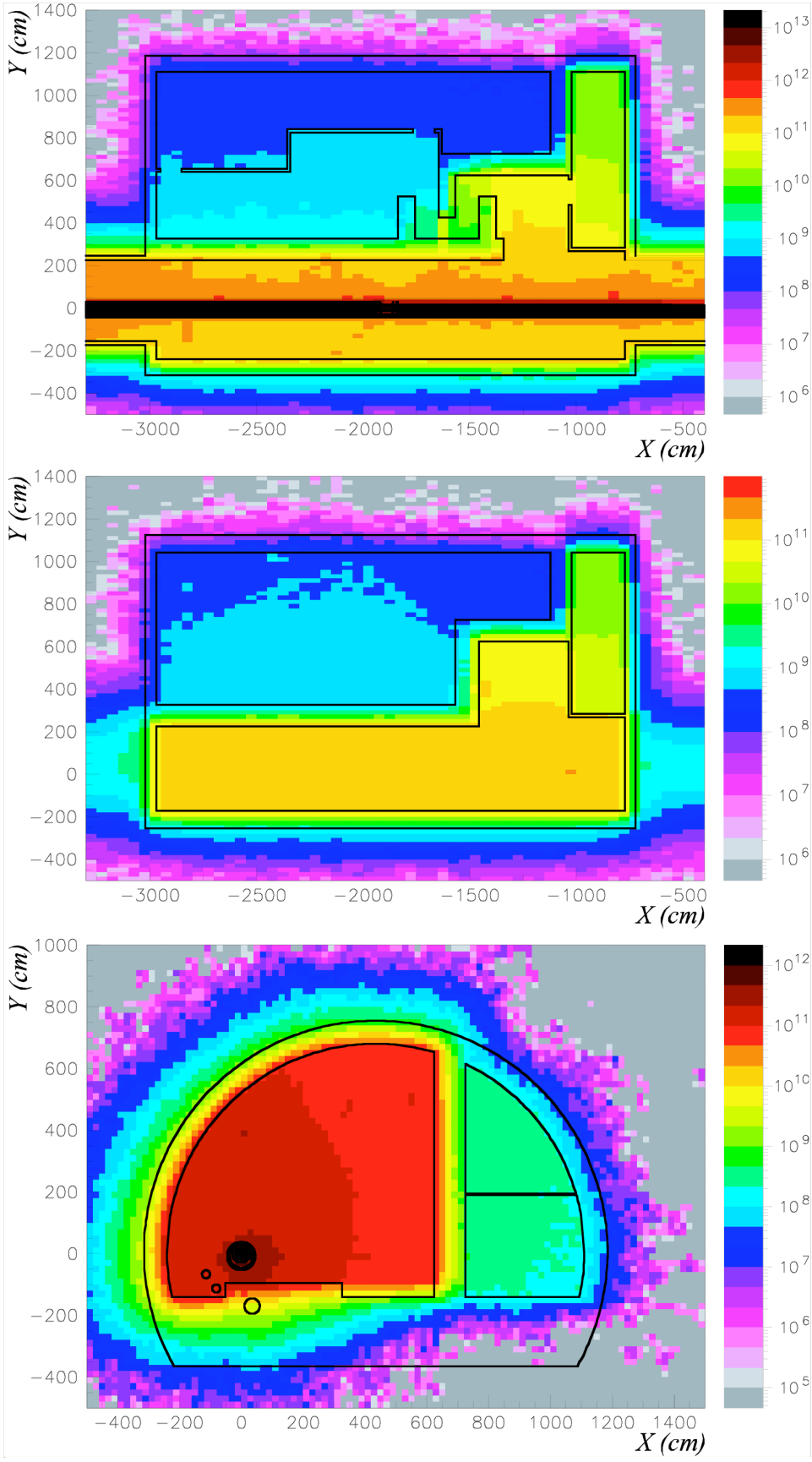

Figure 5 Annual 1 MeV neutrons equivalent fluence. Horizontal cuts averaged over 20 cm about a plane 95 cm above floor levels and vertical cut averaged over 20 cm about section indicated in figure 2.

Appendix A. Gas densities

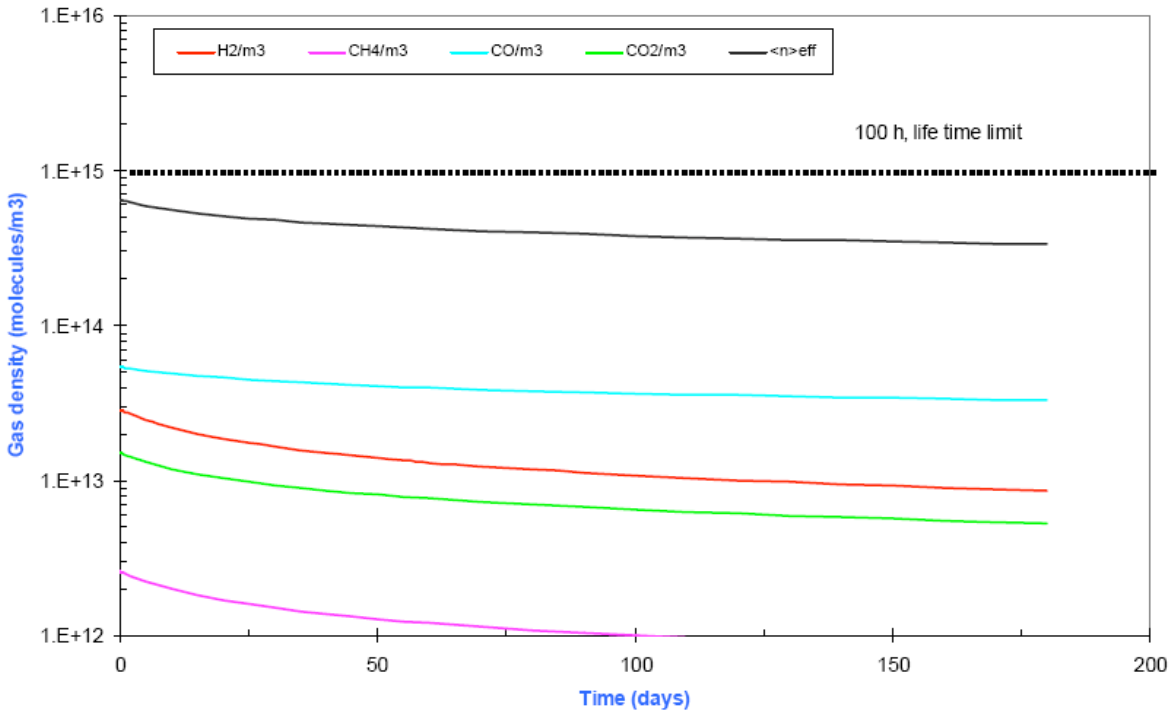

Figure 6. Gas densities in a dipole during LHC physics at 7 TeV

Simulations performed by the vacuum group consider a 10 K cryogenic system at equilibrium i.e. the effective pumping speed of the beam screen is balanced by the cycling desorption of the gases. These take account of the dominant contributions to vacuum instability coming from: 1) beam instability stimulated by ion induced desorption, 2) photon stimulated desorption and 3) electron induced desorption stimulated by the electron cloud.

Once conditioning of the cryo-elements has been performed, according to the adopted model, the LHC operates with nominal parameters. The figure shows the predicted gas density in a dipole at 7 TeV during the first year of physics operation. Considering the relative compositions and the cross-sections shown of each component in the table below it is clear that CO dominates the beam-gas interaction rate. It is convenient for calculation to express the effective gas density of all contributions in terms of H2 molecules. From the figure it is seen that the effective gas density, $\langle n \rangle_{eff}$, starts at ~6 1014 H2/m3 and finishes at ~3 1014 H2/m3 at the end of the year (180 days).

	Start 6E14 H_2/m^3	End 3E14 H_2/m^3	Cross section (mb)
CO	53%	71%	854
H_2	31%	16%	77
CO_2	14%	11%	1317
CH_4	2%	2%	566

Appendix B. Calculation of beam-gas interaction rate from gas densities.

The probability of a beam proton interacting with a residual gas containing n_i molecules of the *i*th molecular species with cross-section σ_i is given by

$$I_{pi} = n_i \sigma_I$$

Calculation is simplified by expressing all densities as H_2 equivalent, $<n>_{eff}$, summing the individual contributions. If we take the already conservative gas density value at the end of the first years physics run as presented in Appendix A we obtain a value close to <n>eff = 3.0×10^{14} H_2/m^3. This yields an interaction probability of 2.32×10^{-15} m^{-1}.

Under nominal physics running conditions the proton fluence per beam is given by

$$N_p = N_0 k_b f$$

Where $N_0 = 1.15\times10^{11}$ is the number of protons per bunch

$k_b = 2805$ is the number of circulating bunches

$f = 11.24$ kHz is the revolution frequency

Here f is calculated from the relation $f_a = hf$ with the harmonic number h equal to 35640 and and the RF frequency f_a equal to 400.8 MHz. This yields a proton fluence of 3.625×10^{18} s^{-1}per beam.

Hence for two beams the beam-gas interaction rate is provided the

$$2\times[I_p N_p] = 1.68\times10^4 \text{ m}^{-1}\text{s}^{-1}$$

Assuming 180 days of physics running per year with fills lasting 27 hours (116 fills) the annual number of beam gas interactions as $1.89\times10^{11}$$m^{-1}$ y^{-1} for both beams.